

New Techniques to Determine Ages of Open Clusters Using White Dwarfs¹

E. J. Jeffery, T. von Hippel, W. H. Jefferys, D. E. Winget, N. Stein, and S. DeGennaro

Astronomy Department, University of Texas at Austin, Austin, TX 78712

ejeffery@astro.as.utexas.edu

ABSTRACT

Currently there are two main techniques for independently determining the ages of stellar populations: main sequence evolution theory (via cluster isochrones) and white dwarf cooling theory. Open clusters provide the ideal environment for the calibration of these two clocks. Because current techniques to derive cluster ages from white dwarfs are observationally challenging, we discuss the feasibility of determining white dwarf ages from the brighter white dwarfs alone. This would eliminate the requirement of observing the coolest (i.e., faintest) white dwarfs. We discuss our method for testing this new idea, as well as the required photometric precision and prior constraints on metallicity, distance, and reddening. We employ a new Bayesian statistical technique to obtain and interpret results.

Subject headings: open clusters and associations: general — white dwarfs: general

1. Introduction

Age measurements are a fundamental problem in astronomy. Understanding the formation sequence of the Galaxy is largely dependent upon accurately knowing the ages of its constituents. There are two main techniques for independently determining the ages of stellar populations: main sequence (MS) evolution theory (via cluster isochrones) and white dwarf (WD) cooling theory. Ages determined from the MS turnoff (MSTO) of globular clusters provide the most reliable age of the Galactic halo (e.g., Chaboyer et al. 1996), while WD cooling ages provide the most reliable age of the Galactic disk (Winget et al. 1987;

¹WIYN Open Cluster Study XXX

Oswalt et al. 1996; Leggett et al. 1998; Knox et al. 1999). Before ages determined by these two techniques can be meaningfully compared, they must be calibrated to the same absolute scale. The best way to do this is to measure and compare WD ages and MSTO ages in several open clusters with a wide range of ages and metallicities.

Cluster WD ages are determined by observing the coolest WDs in the cluster. There is a simple relationship between the cooling time (which is comparable to its total age for the oldest WDs, given their short MS lifetimes) and the luminosity of a WD. Therefore, once the coolest WDs are found, the age of the cluster can be determined. The first studies to apply this technique in open clusters were done by Claver (1995) and von Hippel, Gilmore, & Jones (1995). Later studies (Richer et al. 1998; von Hippel & Gilmore 2000; von Hippel 2001; Claver et al. 2002) showed good agreement in WD ages and MS ages for clusters up to 4 Gyr. A summary of these studies and techniques has recently been presented by von Hippel (2005).

This current technique to derive open cluster ages using WDs is observationally challenging. The coolest WDs are intrinsically faint ($M_V \geq 16$), limiting observations to clusters within a few kiloparsecs, and space-based observations are required for the oldest clusters, particularly to obtain morphological information to remove contaminating background galaxies. To obtain WD ages of more distant clusters (thus increasing the available sample for study), and to reduce the need for space-based observations, we have been motivated to explore new ways to obtain age information from the cluster WDs. One solution is to explore what age information, if any, is available in the brighter cluster WDs.

If successful, the payoff of a technique to derive ages based on only the bright WDs is great. Cluster WD ages will be obtained more routinely because the brighter WDs are easier to observe and deep ground-based data will often suffice. By relying less on space-based data, we will be able to obtain ages for more clusters (as obtaining space-based data is very competitive) which will push our calibration of WD and MSTO ages further. Also, using the bright WDs means that we can observe clusters at greater distances, increasing the number of clusters available for study. This technique would allow WDs to be an increasingly powerful and effective tool for determining ages.

For reasons to be discussed in more detail in the following sections, ages we have derived using the bright WDs are precise, relative ages, rather than accurate, absolute ages. Like other age indicators, we will need to perform extensive calibrations before this age indicator can be used as an absolute chronometer.

This paper is organized as follows: we discuss the rationale behind and techniques used to explore the bright WD idea in Section 2. In Section 3 we present results obtained from our

modeling and Bayesian analysis, as well as present preliminary constraints on the precision and completeness required to obtain good ages. We end with concluding remarks in Section 4.

2. Ages from the Bright Cluster WDs

In Figure 1 we present several color-magnitude diagrams (CMDs) for simulated clusters of varying ages, along with an expanded view of the region of the bright WDs. It is clear from this figure that in the regime of the brighter WDs there are subtle differences in the slope and position relative to the MS of the WD cooling sequences for clusters of different ages. These differences are what make it possible to extract age information without observing to the WD terminus.

2.1. Rationale of the Bright WD Idea

What is the physical reason for the slope differences of the WD cooling sequence in the CMD? Assuming the mapping between a WD’s mass and its MS counterpart’s mass is universal and single-valued, younger clusters have higher mass TO stars, and therefore higher mass bright WDs. The overall mass of a WD affects its position on the CMD; e.g., higher mass WDs have smaller radii and are therefore fainter.

This mapping between a WD’s mass and its MS mass is known as the Initial-Final Mass Relation (IFMR). Ages determined using the traditional cool WD method, as described briefly in Section 1, have little dependence on the IFMR. However, the IFMR greatly affects the hot, bright WDs. The shape and position of the WD cooling sequence relative to the MS in the bright WD regime is a mass effect. Therefore, if there is significant cluster-to-cluster variation in the IFMR, the bright WD technique breaks down. However, it is the general consensus among researchers that the IFMR is single-valued and the same cluster-to-cluster (Weidemann 2000). Because of this dependence on the IFMR, this technique is a relative age indicator. Once the IFMR becomes convincingly single-valued and accurately calibrated, this technique could yield absolute ages.

In Figure 2 we plot just the expanded WD region of Figure 1. Overlaid in this figure are cooling tracks of constant WD mass, i.e., the cooling track of an individual WD with a given (fixed) mass, plotted here for several masses. As illustrated in the figure, the WD isochrones (represented here by various symbols) make a cut across a different combination of WD cooling tracks depending on the cluster’s age, giving rise to differences in slope and

position relative to the MS. As age increases, WDs follow successively lower mass cooling tracks. These differences are what we exploit to derive ages from just the bright cluster WDs.

To state it another way, given a fixed magnitude range, the range of WD masses varies depending on the cluster’s age. In younger clusters, the mass range is much wider in the bright WD regime than it is in older clusters. This mass dependence is the cause of the observed curvature in the WD cooling sequence. The effect is a direct consequence of the IFMR, the mass-radius relation for WDs, and the effect of the Stefan-Boltzmann law in the CMD.

2.2. Testing the Bright WD Idea

In order to explore the age information available in the photometry of the bright cluster WDs, we simulated open cluster CMDs, removed the stars that have been traditionally used for their age information, i.e., the turn off stars and the faintest WDs, and then analyzed the remaining, incomplete CMDs with a new Bayesian algorithm, currently under development by our group (von Hippel et al. 2006). This process is outlined in detail below.

First, we simulated a cluster with a given age, metallicity, distance, and reddening. The simulations incorporate a Miller & Scalo (1979) initial mass function (IMF), MS and giant branch stellar evolution timescales of Girardi et al. (2000), the IFMR of Weidemann (2000), WD cooling timescales of Wood (1992), and WD atmospheres colors from Bergeron et al. (1995). It should be noted that other model ingredients could be used, e.g., a different IMF or a different WD cooling model, but our results would not change since the morphology of the bright WD region in the CMD would remain essentially the same. Additionally we note that all simulated cluster WDs used here are hydrogen-rich, DA WDs. This is an adequate assumption; while 7% of the field WDs are DBs (Kleinman et al. 2004), no DBs have been found in open clusters to date (Kalirai et al. 2005). Although it should be noted that Williams et al. (2006) have recently presented the discovery of a hot DQ (a WD with a He-dominated atmosphere with opacity dominated by atomic carbon) in the open cluster M35. However, even with this discovery, DAs still overwhelmingly dominate non-DAs in open clusters, making our assumption to exclude non-DAs in our simulations a valid approximation.

Our models do not include effects due to residual nuclear burning in the surface layers of the WD. Iben and MacDonald (1986) explored the effects of the mass of the hydrogen surface layer on the luminosity of the WD. They found that the luminosity from nuclear

reactions ($L_{CN} + L_{pp}$) adds very little to the overall luminosity of the star. As the WD cools, the effect is less than or of order 10%. Slight systematic changes to the shape of the WD cooling sequence due to this effect will be higher order for the relative ages we are deriving. As we calibrate the bright WD method to obtain absolute ages, our observations of hot cluster WDs will help us further understand exactly how residual nuclear burning affects the shape of the WD cooling sequence.

Additionally, we have not included field stars in our simulations thus far. This is done mainly for simplicity in the early exploration of the new technique. As we continue to explore the technique and further our simulations, we will incorporate field stars.

After we simulated a cluster, we introduced observational scatter and CMD incompleteness into the simulated cluster. For a given limiting S/N, we calculated Gaussian photometric errors for each star in the CMD. Various values for the S/N and lower M_V (cutoff) were used to allow us to determine the sensitivity of the technique to photometric errors and the level of completeness required to still derive meaningful ages. We will discuss these results more extensively in Section 3. We also imposed an upper M_V (cutoff) = 6 to ensure that our Bayesian algorithm was not able to derive any age information from the MSTO.

Finally, we applied our Bayesian technique to the simulated, scattered, and incomplete CMD. Based on this, MCMC sampled the posterior distribution of the age of the cluster (in log space), as well as the posterior distributions of other cluster parameters, namely metallicity, distance, and reddening. Here, MCMC was set to run for 1,000,000 iterations. The burn in period, that is, the time it takes MCMC to stabilize, was typically 20,000 iterations. Once the posterior distribution of the cluster’s age was sufficiently sampled, we calculated the mean and standard deviation of the posterior distribution and compared these statistics with the known age from the original simulation. (All statistics were calculated using values after the burn in period.)

To understand the dependence of this new technique on various factors (e.g., S/N requirements, CMD completeness requirements, number of WDs required), we ran tests for clusters of several different ages with different photometric precision, CMD completeness, varying number of cluster members, etc. The simulated cluster ages ranging from $\log(\text{age}) = 8.3$ to 9.5 (i.e., 0.2 Gyr to 3 Gyr); all clusters assumed no reddening (i.e., $A_V = 0$), a distance modulus of 0.0^2 , and solar metallicity. In the following section we describe each point tested in detail.

²The distance modulus we chose to use is arbitrary since we apply photometric errors to stars as a function of their absolute magnitude. We chose $(m-M) = 0.0$ so we can consistently refer to absolute, rather than apparent, magnitude.

3. Results

Because we set the age of each simulated cluster, it is straightforward to compare the precision of the MCMC output as a function of various parameters, including limiting S/N, number of WDs, and input precision of other cluster parameters. We discuss each of these points individually below.

Note that throughout we are discussing the precision of the ages obtained with the bright WDs rather than the accuracy. We utilize the morphology of the bright WDs relative to the MS, and as a result, we are not claiming absolute, externally accurate ages. Before that is possible, a calibration of this technique with other techniques (e.g., MSTO ages) must be performed.

3.1. S/N Requirement

We performed tests of the bright WD idea with several limiting S/N levels. This was done in order to understand the dependence of age precision on limiting S/N, and to test if it is possible to obtain acceptable age precision with realistically achievable S/N levels. For clusters of $\log(\text{age}) = 8.3, 8.6, 9.0, 9.3,$ and 9.5 , and given input values of $[\text{Fe}/\text{H}] = 0.0 \pm 0.3$ dex, $A_V = 0.0$ to 0.2 magnitudes, $(m - M) = 0.0 \pm 0.1$ magnitudes, and an M_V (cutoff) = 12, we test age precision versus S/N in Figure 3. The number of WDs in each cluster varied due to the stochastic nature of the simulations.

As expected, precision in age results improved as the S/N increased. These results are encouraging, as it demonstrates that age precision of 20% can be achieved at even the lowest S/N we tested, here $S/N = 15$, and age precision of 10% is achievable by only modestly improving the S/N to 30. Because achieving photometric S/N levels ≥ 100 are difficult, we limited further testing to S/N levels from ≈ 30 to 70^3 .

³ Because achieving photometric accuracy of better than 1–2% is very difficult, we discuss *internal* precision only. The bright WD technique is constrained by the position of the WD sequence relative to the MS; and because absolute photometric errors cause all stars within the CMD to suffer the same offset, the relative position of the WD sequence and the MS will remain the same. Thus, the technique relies most heavily on internal precision rather than external accuracy. Nonetheless, we do not focus on precision better than achievable accuracy levels.

3.2. Required Number of WDs

How many WDs are required for the bright WD technique to yield useful results? To test the dependence of our new technique on the number of bright WDs, we simulated several clusters (all with an age of 1 Gyr and $S/N = 45$ at M_V (cutoff) = 12) with a varying number of WDs populating the hot end of the WD cooling sequence. We present results of the precision in age versus the number of WDs in Figure 4.

As evident in Figure 4, the greater the number of WDs, the better the age precision. These results show that an age precision of 10% can be determined with as few as four WDs.

3.3. CMD Completeness Requirement

So far we have tested the bright WD technique assuming M_V (cutoff) = 12. However, when obtaining real data, the WD cooling sequence may be either more or less complete. We therefore explore the dependence of age precision on CMD completeness. To test this, we simulated several clusters of various ages, imposing incompleteness at $M_V = 11, 12,$ and 13 with a photometric S/N of 45 at M_V (cutoff). Again, the number of WDs in each cluster varied based on the individual simulations.

We show the results in the top panel (A) of Figure 5. The plotted points represent the averages of the results of many individual simulations in that particular location of parameter space; the error bars are the standard deviations of the results. As expected, as the M_V (cutoff) becomes fainter and more WDs are included, the age precision increases. For clusters of 1 Gyr, M_V (cutoff) = 12 (13) typically yields an age precision of $\leq 10\%$ (5%). For younger clusters good results can be achieved even at M_V (cutoff) = 11, e.g., for $\log(\text{age}) = 8.6$, the typical age precision is 10%.

3.4. Precision of [Fe/H] and Other Priors

The Bayesian technique requires prior information on inputs such as distance, metallicity, and reddening. How sensitive are the results to these priors? That is, how precisely do we need to know cluster metallicity, distance, or reddening for the bright WD technique to be useful? In addition to age, the method recovers posterior distributions of metallicity, distance, and reddening. The widths of the posterior distributions of these quantities are substantially narrower than the priors, indicating that all the requisite information is contained in the CMD.

For example, we simulated clusters with an age of 1 Gyr and an M_V (cutoff) = 12. We chose metallicity precisions of 0.1, 0.2, 0.3, 0.4, and 0.5 dex. We display the relationship between age precision and precision of input metallicity in the middle panel (B) of Figure 5. As in the top panel of the figure, the points represent the averages of age results from many simulations with the standard deviations represented by the error bars. Results show little, if any, dependence between the prior precision on metallicity and the age determined from the bright WDs. This does not mean that cluster metallicities are unimportant in this work. On the contrary, we hope to eventually test cluster MS ages versus cluster WD ages at a range of metallicities. Rather, good cluster metallicities are not required for a precise bright WD age.

3.5. Age Range

As mentioned in Section 2.1, as a cluster ages, the slope of its WD cooling sequence becomes increasingly indistinguishable from other old clusters. Because of this, we desired to understand how the precision of the bright WD age varied as a function of increasing age. We show the results of this in panel C of Figure 5. We have not yet tested any ages older than $\log(\text{age}) = 9.5$ (i.e., 3 Gyr) due to limitations in our input models; however, as we incorporate more high mass WD cooling models, we will continue to push this technique to greater ages.

We display the results in the bottom panel (C) of Figure 5. As usual, the points are the averages of several simulations with the standard deviations given by the error bars. Based on this figure, we see that for the ages tested, the age precision of the bright WD technique does not significantly decrease with increasing age. Further testing will be done to determine this effect for clusters of ages above 3 Gyr, placing an important constraint on the technique.

As the age of a cluster increases, two main factors contribute to the age precision. The first is that as the cluster becomes older, there are more WDs. As demonstrated in Section 3.2 (particularly Figure 4), as the number of WDs increases, so does the age precision. Competing with this effect is that as the cluster ages, the bright portion of its WD cooling sequence becomes increasingly difficult to distinguish from other old clusters (see Figures 1 and 2). It is possible that there exists a “sweet spot,” where these two effects complement each other and contribute to a very precise age. This may be the cause of the sudden tightness in age precision around $\log(\text{age}) = 9.3$ in Figure 5. However, as a cluster increases in age, the number of WDs quickly begins to do little to improve age precision while the WD sequences become more and more degenerate. Further testing, particularly expanding tests out to older clusters, will more clearly help us understand this effect and constrain the

bright WD technique.

4. Conclusions

Current observational techniques to obtain ages from cluster WDs are challenging, due to the faintness of the coolest cluster WDs. We have shown that the bright WDs can be used to determine cluster ages. This is done by exploiting the differences in slope and position relative to the MS of the WD cooling sequence in the regime of the bright WDs caused by varying WD mass distributions. By employing a new Bayesian technique to fully extract all age information in the WD portion of the CMD, we have shown that there is sufficient age information in the bright WDs.

With the assumption of a single-valued IFMR, our studies show that we can achieve age precision of 10% with a $S/N \geq 30$ at M_V (cutoff) = 12, with as few as 4 WDs for low reddening clusters. We find no dependence of age precision on the prior precision of metallicity, distance, and reddening, nor on the age of the cluster, at least up to the oldest age (3 Gyr) tested in this study. Additional studies will be done to determine if this technique is feasible for even older ages, particularly ages comparable to those of the globular clusters.

If the bright WDs technique continues to be successful in determining precise cluster ages, WD cosmochronometry can be applied to more distant and/or older clusters (where observing to the WD terminus is especially challenging). This will increase the sample of objects available for study, particularly allowing us to sample clusters in age-metallicity space that would be otherwise too difficult using the current method of determining WD ages. This technique will allow WDs to be an increasingly powerful and effective tool for studying the ages of stellar populations.

This material is based upon work supported by the National Aeronautics and Space Administration under Grant No. NAG5-13070 issued through the Office of Space Science, and by the National Science Foundation through Grant AST-0307315.

REFERENCES

- Bergeron, P., Wesemael, F., & Beauchamp, A. 1995, *PASP*, 107, 1047
- Chaboyer, B., Demarque, P., & Sarajedini, A. 1996, *ApJ*, 459, 558
- Claver, C. F. 1995, PhD Thesis, The University of Texas at Austin

- Claver, C. F., Liebert, J., Bergeron, P. 2001, *ApJ*, 563, 987
- Girardi, L., Bressan, A., Bertelli, G., & Chiosi, C. 2000. *A&AS*, 141, 371
- Iben, I. & MacDonald, J. 1986, *ApJ*, 301,164
- Kleinman, S.J., et al. 2004, *ApJ*, 607, 426
- Kalirai, J.S., Richer, H.B., Hansen, B.M.S., Reitzel, D., & Rich, R.M. 2005, *ApJ*, 618, L129
- Knox, R.A., Hawkins, M.R.S., & Hambly, N.C. 1999, *MNRAS*, 306, 736
- Leggett, S.K., Ruiz, M.T., & Bergeron, P. 1998, *ApJ*, 497, 294
- Miller, G. E., & Scalo, J. M. 1979, *ApJS*, 41, 513
- Oswalt, T.D., Smith, J.A., Wood, M.A., & Hintzen, P. 1996, *Nature*, 382, 692
- Richer, H.B., Fahlman, G.G., Rosvick, J., & Ibata, R. 1998, *ApJ*, 504, L591
- von Hippel, T. 2001, in *ASP Conf. Ser. 245*, ed. T. von Hippel et al., (San Fransisco: ASP), 190
- von Hippel, T. 2005, *ApJ*, 622, 565
- von Hippel, T., Gilmore, G. 2000, *AJ*, 120, 1384
- von Hippel, T., Gilmore, G., & Jones, D.P.H. 1995, *MNRAS*, 273, L39
- von Hippel, T., Jefferys, W. H., Scott, J., Stein, N., Winget, D. E., DeGennaro, S., Dam, A., & Jeffery, E. J. 2006, *ApJ*, 645, 1436
- Weidemann, V. 2000, *A&A*, 363, 647
- Williams, K. A., Liebert, J., Bolte, M., Hanson, R. B. *ApJ*, 643, L127
- Winget, D. E., Hansen, C. J., Liebert, J., van Horn, H. M., Fontaine, G., Nather, R. E., Kepler, S. O., & Lamb, D. Q. 1987, *ApJ*, 315, L77
- Wood, M. A. 1992, *ApJ*, 386, 539

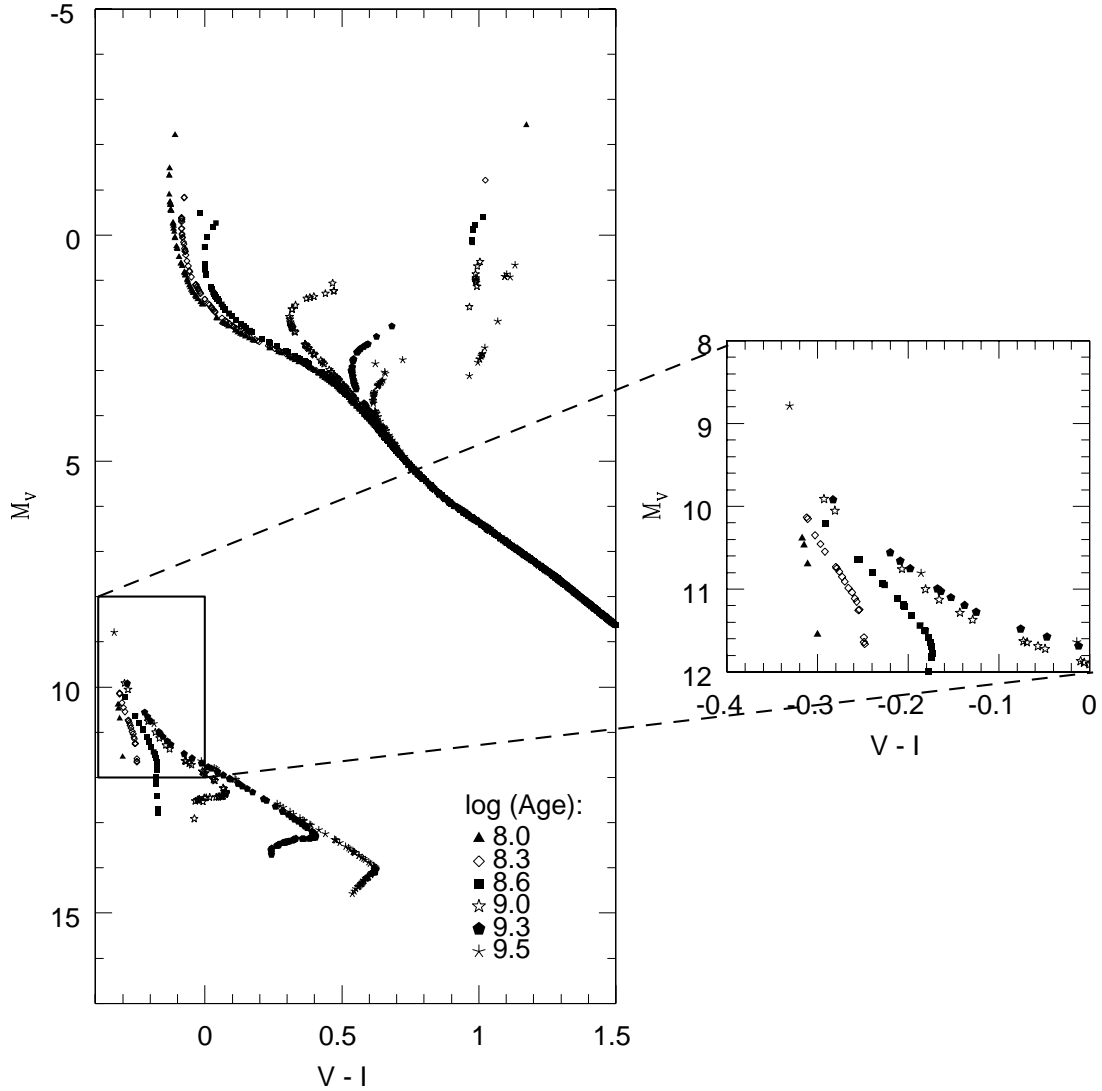


Fig. 1.— Simulated clusters for several different ages. The expanded region shows the regime of the brighter WDs, clearly showing the subtle differences in the slopes and positions of the WD cooling sequences relative to the MS for clusters of different ages. This makes it possible to extract age information without observing the faintest WDs.

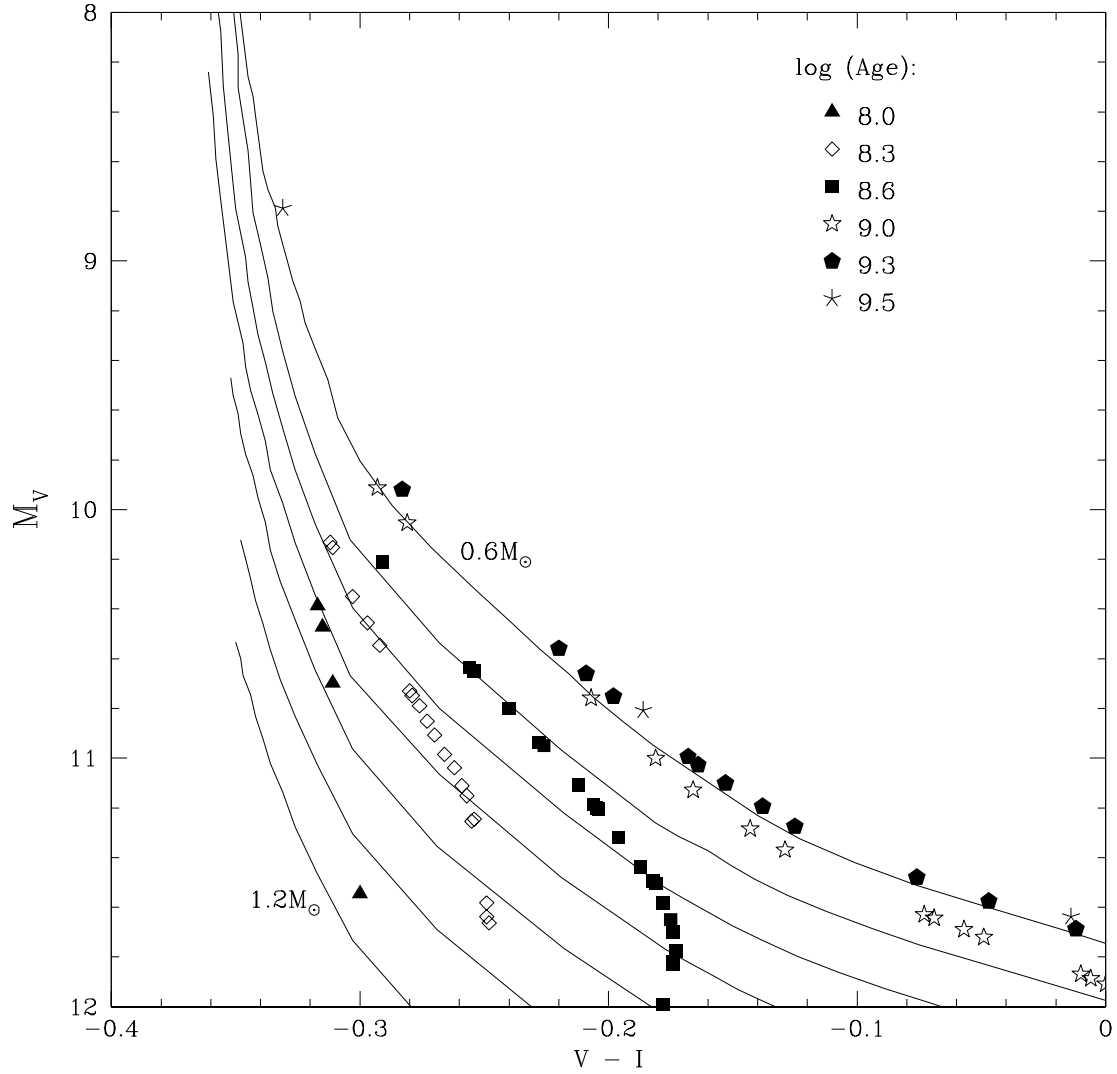


Fig. 2.— WD region of the CMDs from Figure 1, with cooling tracks for constant WD mass overlaid. As age increases from 10^8 years (solid triangles) to 3×10^9 years (asterisks), WDs follow tracks of lower and lower mass.

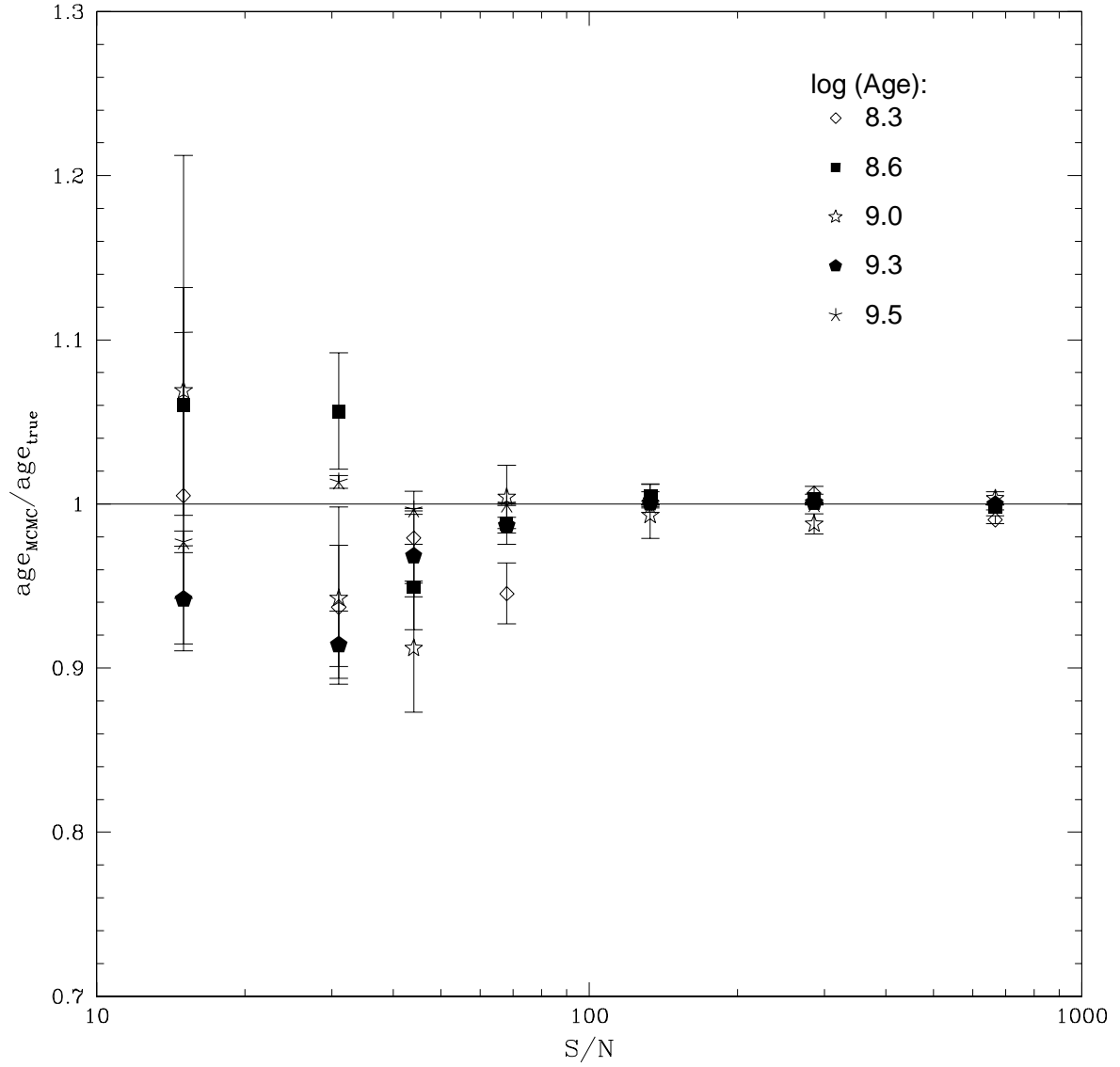


Fig. 3.— Relationship between the true cluster age (age_{true}), the mean of the age distribution obtained via MCMC (age_{MCMC}), and the S/N for M_V (cutoff) = 12. The error bars represent the standard deviation in the posterior distribution.

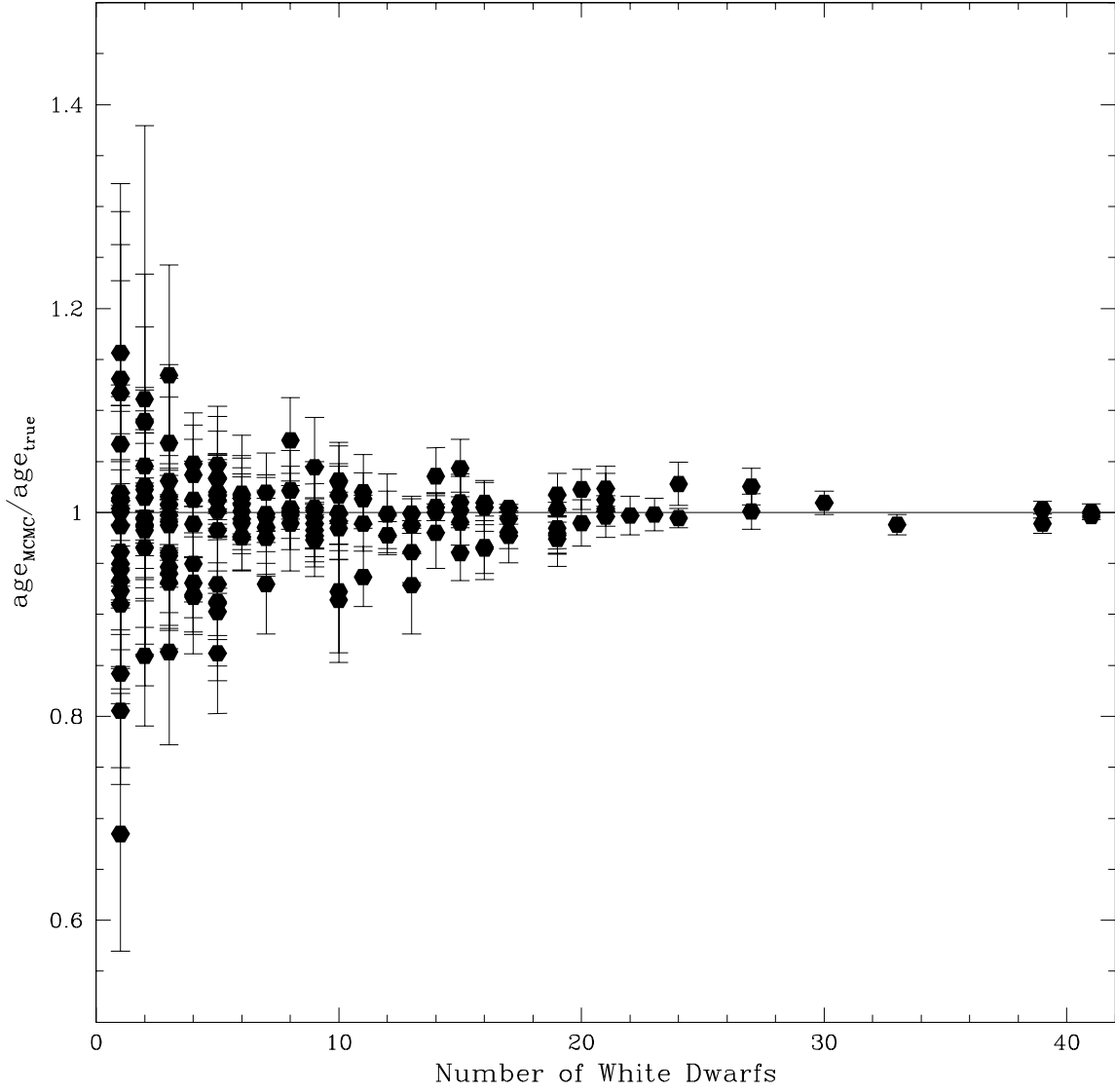


Fig. 4.— Relationship between the true cluster age, the mean of the age distribution obtained via MCMC, and the number of WDs observed.

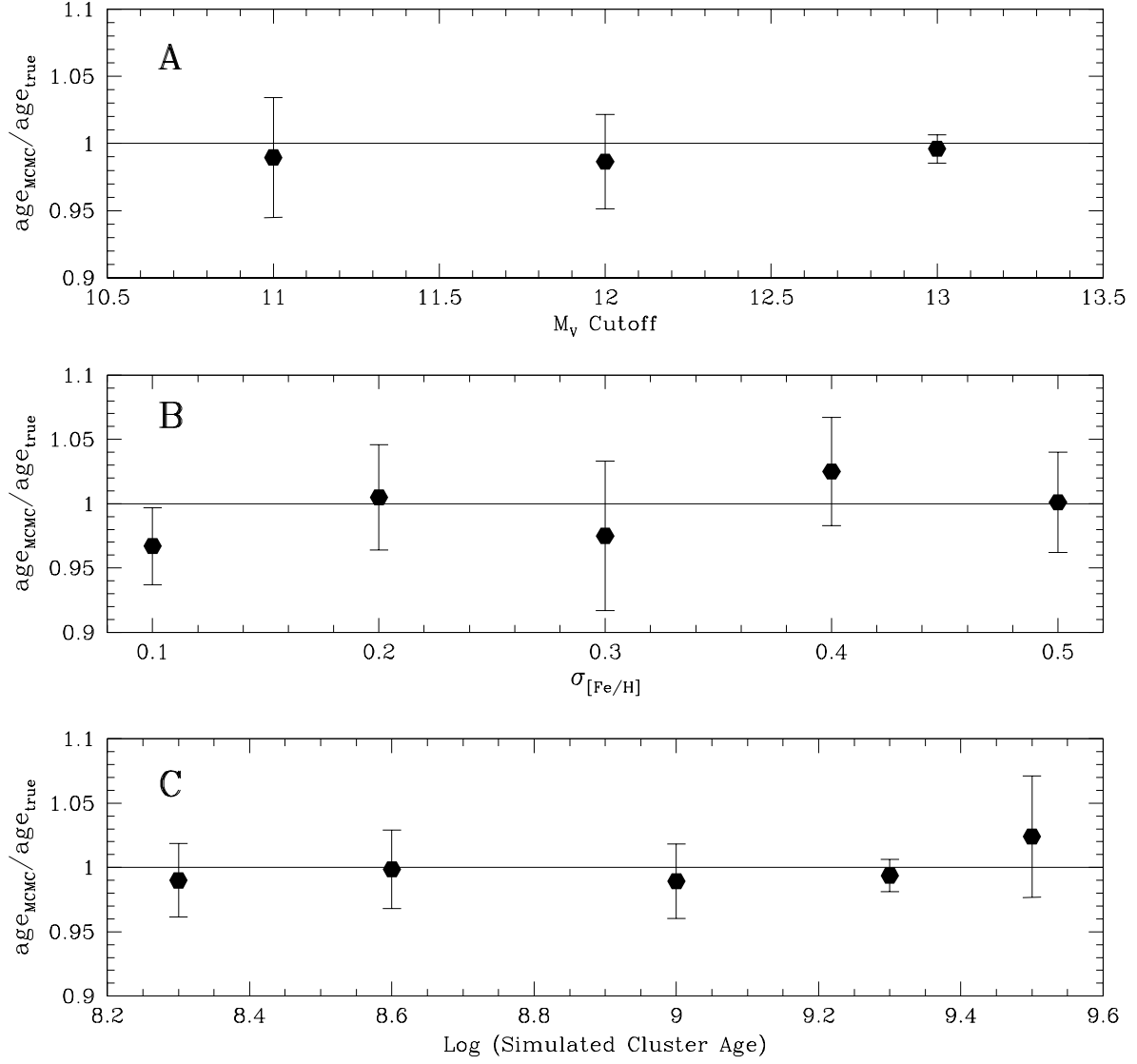


Fig. 5.— Relationship between the true cluster age, the mean of the age distribution obtained via MCMC, and (A) the CMD completeness, (B) prior precision of the cluster metallicity, and (C) the simulated cluster age.